NOVATEUR PUBLICATIONS
INTERNATIONAL JOURNAL OF INNOVATIONS IN ENGINEERING RESEARCH AND TECHNOLOGY
[IJIERT] ISSN: 2394-3696 Website: ijiert.org
VOLUME 8, ISSUE 6, June. -2021

OPTIMIZATION OF FLOATING HORIZONTAL AXIS WIND TURBINE (FHAWT) BLADES FOR AERODYNAMIC PERFORMANCE MEASUREMENT

Sajid Ahammed
School of Engineering, UOW Malaysia KDU University College,
Utropolis Glenmarie, ShahAlam, Malaysia.
* 0116915@kdu-online.com

ABSTRACT

Wind power is one of the most important sources of renewable energy which extract kinetic energy from the wind. Currently much research has concentrated on improving the aerodynamic performance of wind turbine blade through wind tunnel testing and theoretical studies. However, wind turbine simulation through Computational Fluid Dynamics (CFD) software offers inexpensive solutions to aerodynamic blade analysis problem. The purpose of this paper is to find the effect of angle of attack towards the blade of Floating Horizontal Axis Wind Turbine (FHAWT) and optimize to get the best blade performance in between twisted and untwisted blade which will give maximum lift and drag force ratio. The optimization of the FHAWT blades are carried out by analysing, modelling and simulation by using simplified spreadsheet method, CFD analysis in ANSYS WORKBENCH 2020 R1 software and wind tunnel testing. The blades are evaluated regarding their lift and drag force ratio in different angle of attack and wind speed. The results, obtained from both computer programs, wind tunnel testing and the initial hand calculations, are comparable and satisfying. Finally, the model was implemented to optimize blades performance, especially at low wind velocities, which is crucial to produce power during operating in offshore environment.

Keywords: Aerodynamic, Angle of Attack, Optimization, wind tunnel, Lift force, drag force.

INTRODUCTION

In this modern world to generate electricity from offshore wind turbines has become famous by the Floating Horizontal Axis Wind Turbine (FHAWT)[1]. Wind turbine is a device that converts wind energy from kinetic energy to electrical energy. There are two types of wind turbine which is vertical axis wind turbine (VAWT) and horizontal axis wind turbine (HAWT). In figure 1-1 the difference between HAWT and VAWT has shown [2].

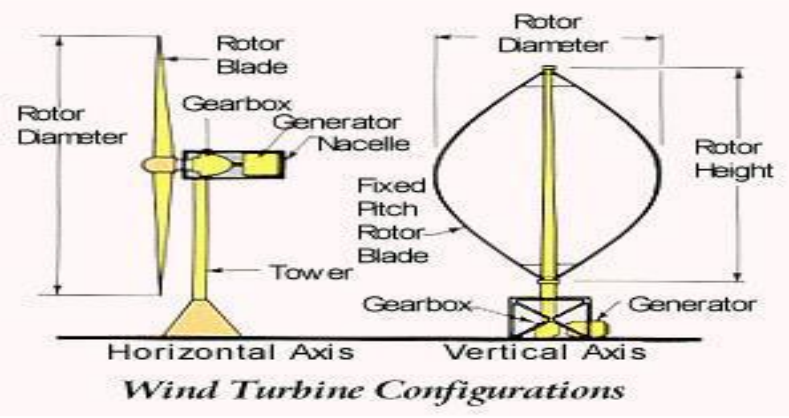


Figure 1.1: HAWT VS. VAWT Design [2].

While designing the Floating Horizontal Axis Wind Turbine (FHAWT) blade profile, blade taper, tip loss, variable wind speed and angle of attack place an important role. The angle of attack plays an important role towards the blade of wind turbine which should be investigated and optimized to get the best performance of FHAWT. When the wind turbine operates in wind flows, the angle of attack (AOA) of a given blade varies

at different azimuths. The AOA of the blade is one of the most dominating parameters for the wind turbine control and the blade design. As the AOA fluctuates in flows, the aerodynamics of the operating wind turbine is significantly influenced. On the one hand, the aerodynamic loads of the blades are closely related to the AOA. At each blade section, the aerodynamic forces are calculated based on the AOA and the inflow velocity. Generally, the lift force increases with the AOA in the attached flow state while decreases with the further increase of the AOA once the stall angle is exceeded. The blades suffer from larger aerodynamic loads and bending moments since the blades experience larger increase in lift due to the dynamic stall. The low efficiency due to low lift and drag ratio is one of the main problem found in FHAWT.

To find out the best blade performance between twisted and untwisted blade and which will give the maximum lift to drag force ratio lift was measured directly from the force balance. It is known that the maximum power efficiency is achieved when the blade is twisted according to a program that depends upon the variation of the sectional lift and drag coefficients with angle of attack. Results for a typical air foil cross-section show that the optimum angle of attack and optimum twist angle of the blade improves the performance of the wind turbine.

METHODOLOGY

The process started with brainstorming and getting the idea of FHAWT. After that need to select the air foil for FHAWT and considering the designing parameter. Then need to design the turbine and floating platform. After that need to finalize the platform and whole turbine design. Then simulation of FHAWT will be done in ANSYS. Then can analyze and compare the optimization of FHAWT. If the result shows the optimization done, then the aim and objective will be achieved. After that need to fabricate the FHAWT. Optimization of FHAWT is done. The flow chart of methodology is given in Figure 2.1

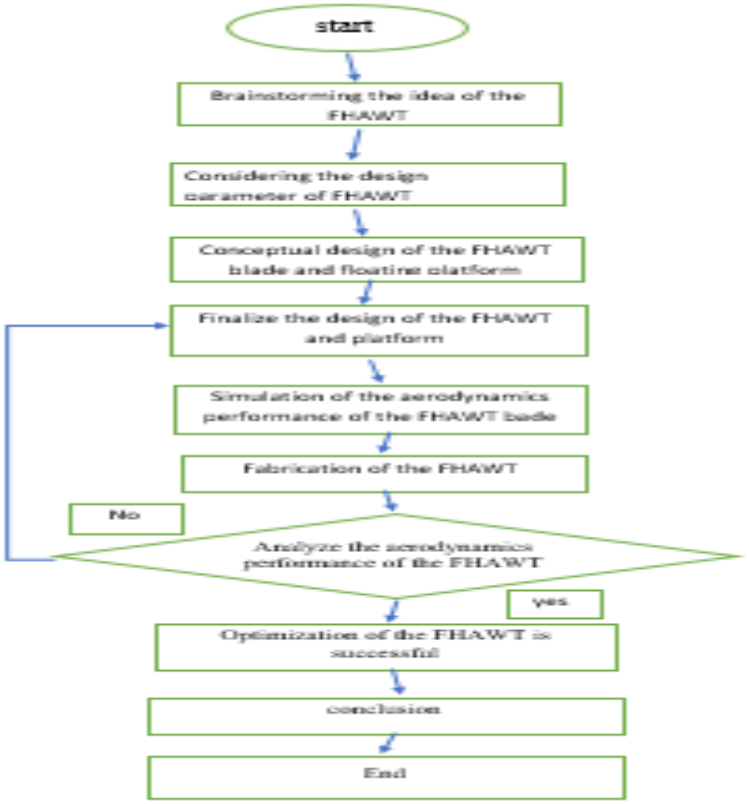


Figure 2.1 The flow chart of methodology

2.1 Design procedure outline

There is a ramification of various techniques that may be taken in wind turbine layout and therefore there are also some of issues that need to be taken into account. The layout method outlined in "(McGowan, 2003), sets tips for the layout of a wind power converter and has been taken into consideration for application in this venture.

2.2 Air foil selection

Mach range and Reynolds number need to be defined, before introducing the airfoil behavior. Mach number is a ratio of speed of an object over, Sound and its speed defined as following equations [3] :

$$Ma = \frac{v_s}{u_c}$$

Where Ma is Mach number, vs is object speed and uc is sound speed. Subsonic is defined as, transonic is defined as, supersonic is defined as and hypersonic is defined as. Mach<=1, transonic is Mach =1, supersonic is Mach >=1, hypersonic Mach >=5

The Reynolds number is a non-dimensional value and it is a ratio of inertial force to viscous force, defined as:

$$\mathrm{Re} = \frac{\rho V^2 / L}{\mu V / L^2} = \frac{\rho V L}{\mu}$$

Aerofoil behavior can be described into 3 float regimes: the attached float regime, the high lift/stall improvement regime and the flat plate/completely stalled regime [4]. According to Witcher, Witcher and Harding for efficient blade will have high lift to drag ratio. NACA 4- digit series will have given the good performance at low speed. Therefore, choose the NACA 6409 blade air foil for analysis. These profiles given the better performance at low speed having high lift to drag ratio and good stall properties. Specification of NACA 6409 [5] low speed wind blade profile –

- Max thickness 9% at 29.3% chord.
- Max camber 6% at 39.6% chord Source [6]

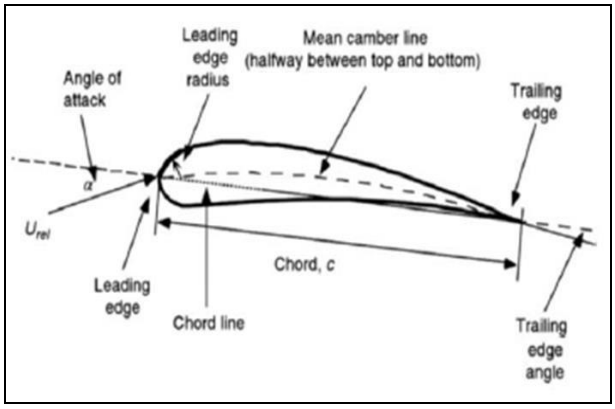


Figure 2.2: Air foils important parameters[5]

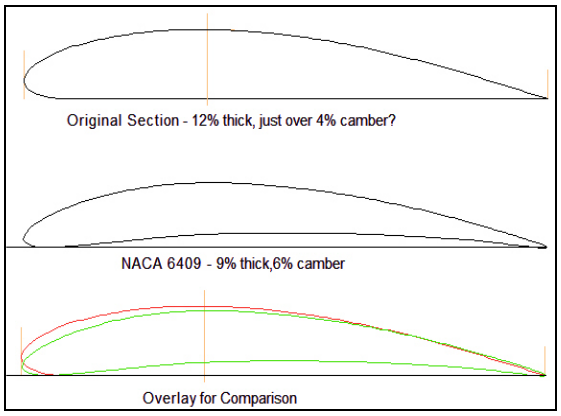


Figure2.3: NACA 6409 Comparison [6]

Modelling and Analysis

The design process of the blade design of FHAWT has several steps. Where the blade will be redesigned by using NACA 6409 air foil. The air foil coordinates have taken form Air Foil tools official website[5]. And the data used for designing the blade such as cord length, angle of twist and the ratio of r/R has been taken from the previous research paper by McGowan, Rodgers.[7]

Table 3.1 Twist and chord distribution for a twisted blade [7]

No	r/R	Twist angle (deg.)	Chord length, (l)
1	0.1	38.2	1.375
2	0.2	20	0.858
3	0.3	12.2	0.604
4	0.4	8	0.462
5	0.5	5.3	0.373
6	0.6	3.6	0.313
7	0.7	2.3	0.269
8	0.8	1.3	0.236
9	0.9	0.6	0.210
10	1	0	0.189

By using the NACA 6409 air foil coordinates the three-dimensional air foil will be created in the solid works. At first after starting the solid works need to select the front plane, then from reference geometry select plane then create ten planes the distance between one plane to another plane will be 15.94mm. After that from reference geometry need to select the curve through xyz plane then input the following coordinates in the table given below. Then the air foil NACA 6409 will be created in solid works window in Figure 3.4. After that need to select plane 1 and click edit button then need to convert the 3d air foil to 2d air foil in Figure 3.5. By using same procedure ten air foil will be created in ten planes where the angle of twist and cord length will be given according to the date given in Table 3.2.

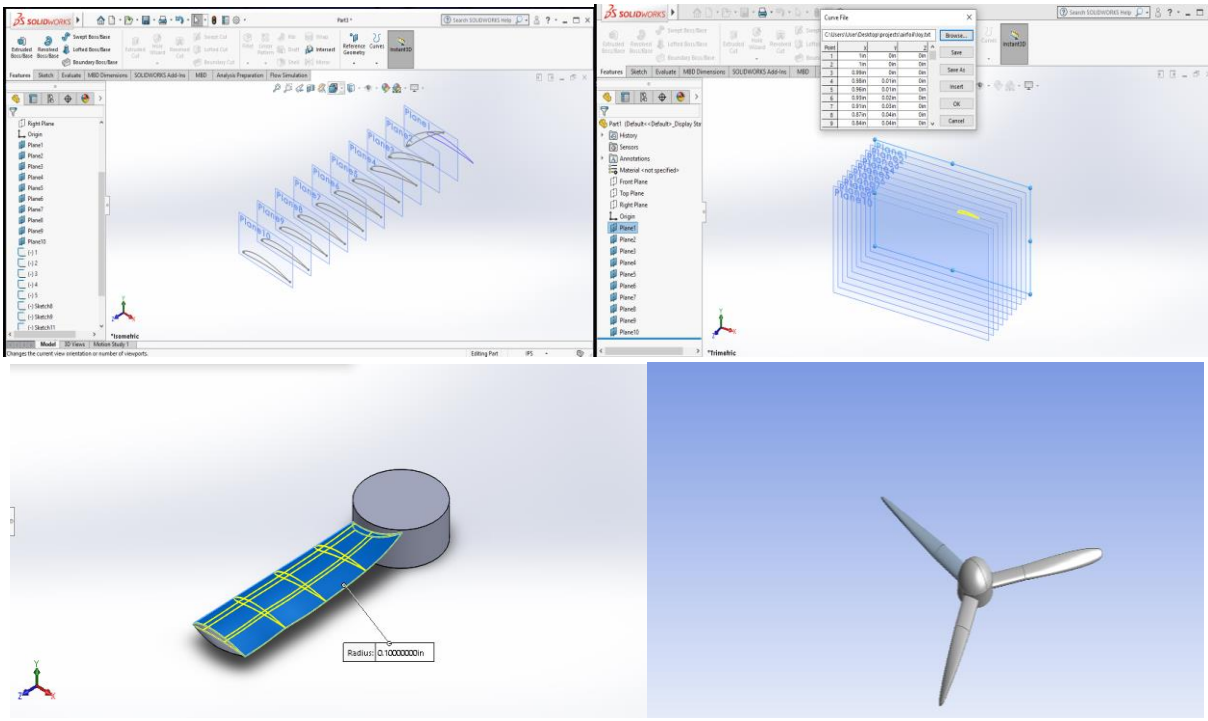


Figure 3.1: Modelling process of FHAWT

The twisted blade FHAWT shown in Figure 3.16, where solid works model and engineering drawing are shown with all dimension

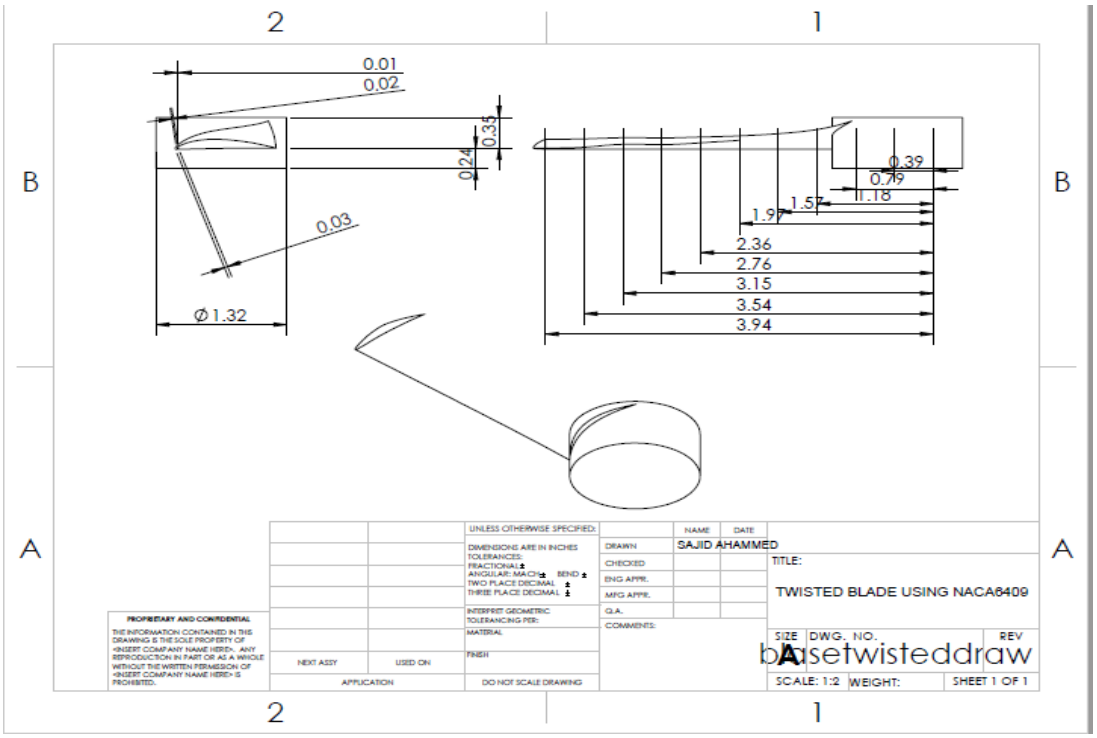


Figure 3.2 Engineering drawing of twisted blade of FHAWT

RESULT AND DISCUSSION

This chapter presents results from physical characterization tests (wind tunnel test), theoretical calculation and ANSYS simulation data of the twisted blade of FHAWT turbine. The collected performance data will then be compared to target performance curves and suggestions for a future model blade design will be given. Firstly, theoretical calculation will be done by using the porotype data of the FHAWT to find drag and lift forces at the speed of wind tunnel testing. Then simulation will be done in ANSYS WORKBENCH 2020 R1 software to find drag and lift forces of the model. Lastly the designed FHAWT twisted blade will be tested in the wind tunnel and after that the lift force and the drag force will be collected at different angle of attack and wind speed. The three different values will be compared to see the errors and the precisions of the collected data. After that the errors of data among these experiment will be calculated to see the preciseness of the data. Then the graph will be plotted and compared with the existing untwisted FHAWT's blade and find the best performance. The lift and drag force for FHAWT blades will be calculated from the representative equation which are given below

$L = \frac{1}{2} C_L \rho v^2 A$ …… (1) and $D = \frac{1}{2} C_D \rho v^2 A$ ……. (2)

Where, L = lifting force (N), D = drag force (N),
C_D = drag coefficient, C_L = lifting coefficient,
ρ = density of fluid (kg/m^3), v = flow velocity (m/s),
A = body area (m^2).
Now from equation can calculated the lift and drag force for the blade with the data of FHAWT blades.

Calculation of FHAWT:

4.1.1 Lift force

From Equation 1
L = ½ CL ρ v2 A
Where,
CL = 0.039 [For NACA6409 Aerofoil specific section] [5]
ρ = 1.225 kg/m^3
A= πr2 = 3.1416× (0.1135) [r = radius of blade attacked by wind flow
= 0.0405 m2 =227mm×1m2×1000mm = 0.1135 m]
V= 36.5 m/s
Then,
L =0.039×1.225× (36.5)2×0.0405 2 =1.28 N

4.1.2 Drag force

From Equation 2
D =½CD ρ v2 A
CD= 1.72× 10-3 [For NACA6409 Aerofoil for specific section] [5]
ρ = 1.225 kg/m^3
A= πr2 = 3.1416× (0.1135) [r = radius of blade attacked by wind flow 83
= 0.0405 m2 =227mm×1m2×1000mm = 0.1135 m]
V= 36.5 m/s
Then,
D =1.72× 10−3×1.225× (36.5)2×0.0405 2 =0.056N

4.2 Simulation in ANSYS of FHAWT:

After running the calculation and completing 200 calculations the following iteration graph has been plotted in the fluent window. Figure 5.0 shows the residual velocity graphs for 200 iterations in direction of continuity, (x, y & z)-velocity, k and omega.

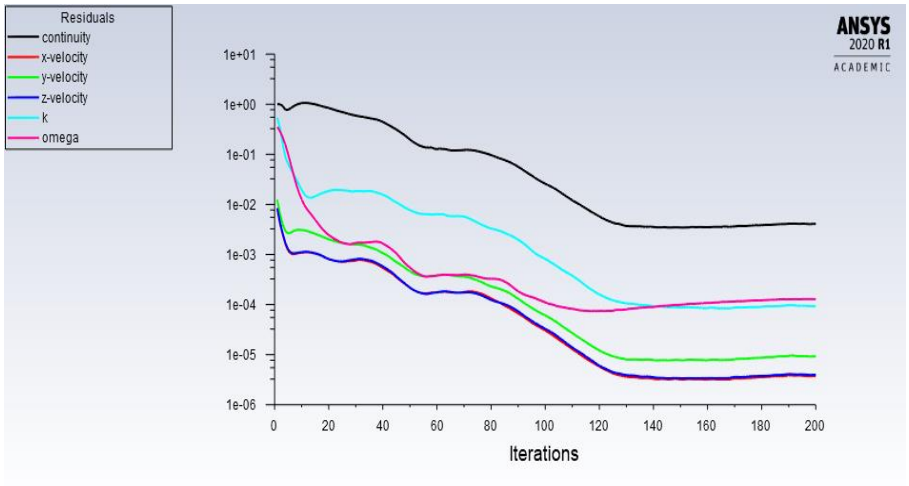


Figure 4.1: Residual velocity graphs of 200 iteration

4.2.1 Lift force plot

The lift force is plotted in the new window of the Workbench window and shows the result of lift force vs iteration. Where it can see that the maximum lift for can get around 1.16N and the minimum lift force is around -0.18N. The value varies between -0.18N-1.16N. The lift force is higher at 85 iteration point and after 100 iterations it stays constant because of the constant balanced wind flow (can see from velocity contour plot in next section 5.2.3) among the FHAWT blades. The average lift force after 90 iterations is around 1.05N. do it is clear that when the velocity is constant and it attacks to blade evenly then the lift force of the blades keeps constant as well. So the higher wind creates high lift force to the blade.

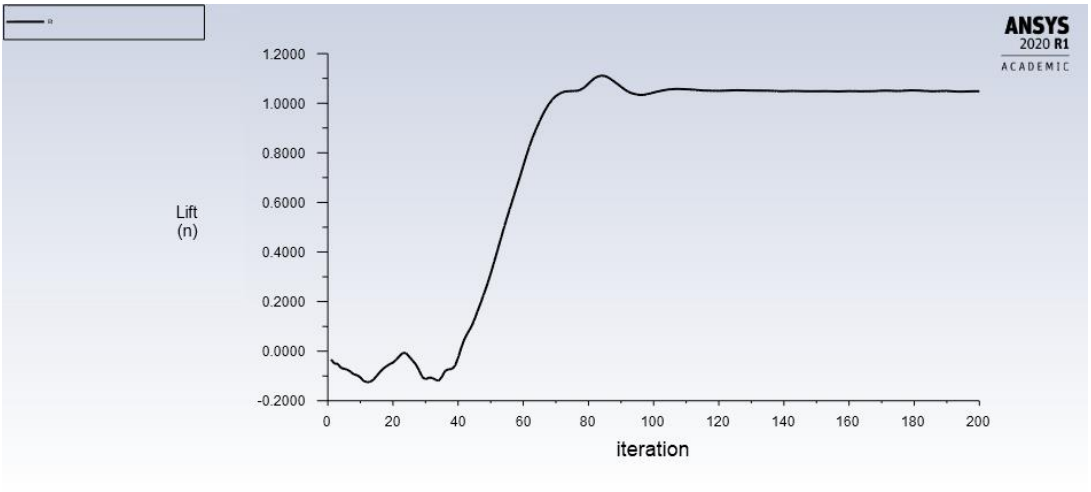


Figure 4.2: Lift force vs. iteration graph IN ANSYS Fluent simulation.

4.2.2 Drag force plot

From the graphs it has seen that it is completely opposite of lift force graph. It is opposing the wind to pass through the blades that's why the values are negative. It changes with velocity of the wind and completely opposite of lift force. When the lift force is high then the drag force is high as well. But because of the twist distribution of the blade the drag force is quite low. Where the values vary from -0.034N to 0.07N. the maximum drag force can get at 85 iteration point which is around -0.07N and minimum at beginning which is around -0.034. the 100 iteration drag force becomes stable as well. Though it is totally opposite graph of lift force but act similarly with the changes of iteration. The result mainly shows the low drag force than the lift force.

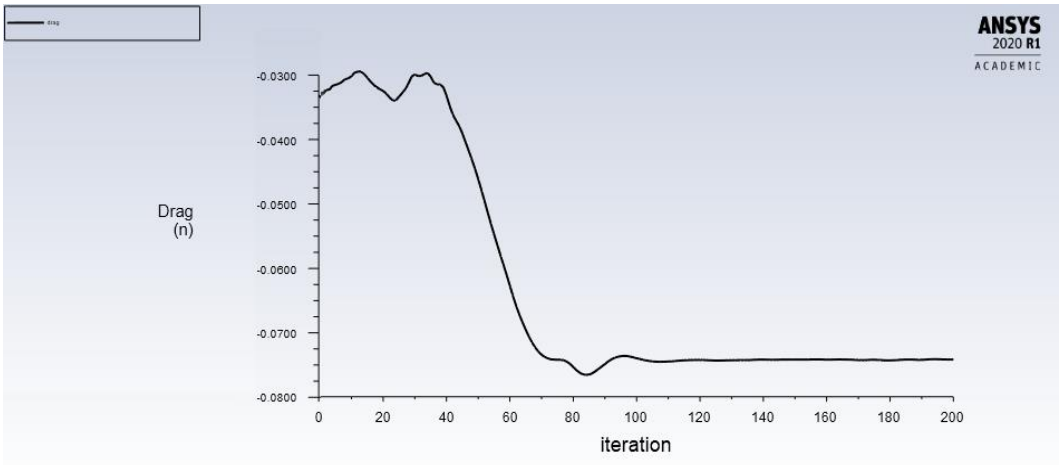


Figure 4.3: Drag vs. iteration graph IN ANSYS Fluent simulation.

4.2.3 Contour plot

I. Velocity magnitude plot

Figure X and Y illustrates the isometric and top view of FHAWT blades plot, where it shows that when hits the blade because twisting angle of the blade it can pass through easily and generate maximum lift force. As the figure shows that the edge of the blade is highly affected to produce high lift force where the drag force reduced. At the edge of the blade the velocity magnitude is around 1.35×10^2 m/s which is maximum. It is known from equation 5.1.1 that lift force is directly proportional to velocity. When the velocity is maximum the lift force will be maximum as well.

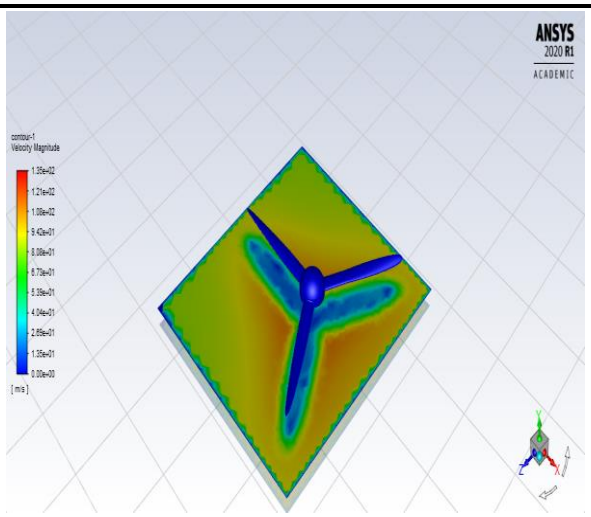


Figure 4.4: Velocity magnitude plot of FHAWT blades

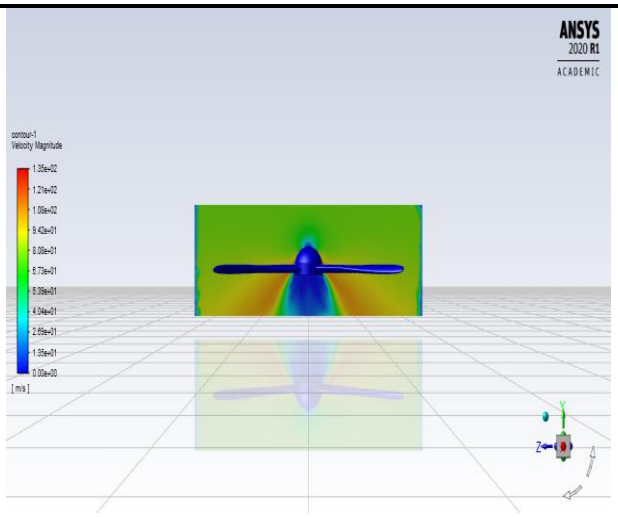


Figure 4.5: Top view of velocity magnitude plot.

Static Pressure Plot

Form Figure Z can come to an explanation that the static pressure acting on the blades in very less area and the area affected by maximum static pressure which is around 8.26×10^3 Pascal. It can also be noted that at the front and edge of the blade low pressure distribution is observed because of twisted blade. It can attribute that reverse flow and low pressure regions generated due to the twisted blade profile so the drag will be less.

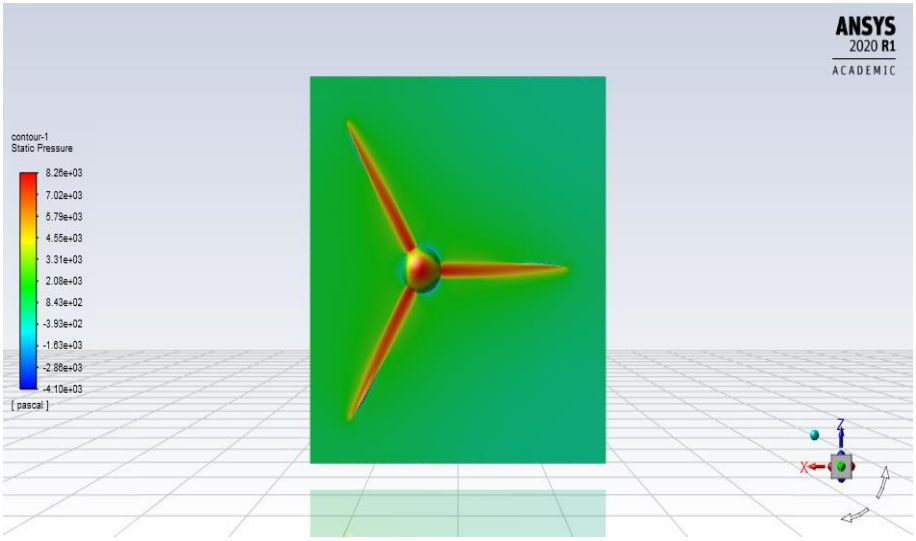


Figure 4.6: Static pressure contour plot of FHAWT blades

4.3 Wind tunnel test of FHAWT

The testing of the FHAWT blade has been done in AF100 subsonic wind tunnel where the blades lift and drag force has been collected in different velocities and angle of attack. Where (0,10,20,30,40,50,60,70 and 80) mmH_2O dynamic pressure has been chosen and angle of attack (-10, -5,0,5,10,15,25 and 30) ° has been selected to find the aerodynamics performance.

4.3.1 Wind tunnel testing data

The wind tunnel test has been performed in the velocity range and different angle of attack (-10, -5,0,5,10,15,25 and 30) °. For different velocity and angle of attack the collected aerodynamic performance data are shown in the table which is given below. Table 4.1 shows the data of lift and drag force at different

angle of attack at wind speed 18.23m/s. Where lift force, drag force, pitching moment and L/D ratio has tabulated and shows the relation with velocity and angle of attack.

Table 4.1: Lift different angle of attack at wind speed 18.23m/s

No	Angle of attack, (°)	Lift (N)	Drag (N)	Pitching moment (Nm)	Lift and drag ratio, L/D
1	-10	0.38	0.02	0.02	19
2	-5	0.37	0.03	0.03	12.33
3	0	0.21	0.01	0.01	21
4	5	0.24	0.02	0.02	12
5	10	0.41	0.02	0.03	20.5
6	15	0.24	0.03	0.02	8.0
7	25	0.31	0.02	0.03	15.5
8	30	0.29	0.03	0.03	9.67

Figure 4.7 shows the graph of lift and drag vs angle of attack at wind speed 18.23m/s. Where the maximum lift force is at 10° and minimum is at 0°. The maximum lift force is at 15° and minimum is at 0°. The drag and lift force both changes at different angle of attack and velocity as well. The following Figure 4.8 shows a relationship graph between L/D against angle of attack where the maximum L/D ratio can get around 20.5 at 10° angle of attack and minimum at 30°.

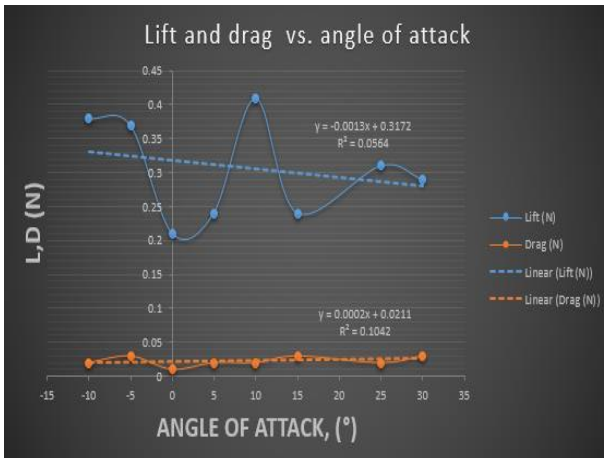


Figure 4.7 Lift and drag vs angle of attack at 18.23m/s

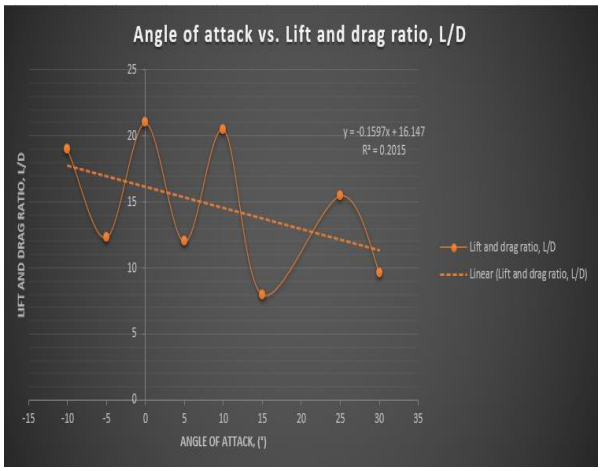


Figure 4.8 Lift and drag ratio vs angel of attack at 18.23m/s

Table 4.2 shows the data of lift and drag force at different angle of attack at wind speed 18.23m/s. Where lift force, drag force, pitching moment and L/D ratio has tabulated and shows the relation with velocity and angle of attack.

Table 4.2: Lift and drag force at different angle of attack at wind speed 22.33m/s

No	Angle of attack (°)	Lift (N)	Drag (N)	Pitching moment (Nm)	Lift and drag ratio, L/D
1	-10	0.53	0.02	0.03	26.5
2	-5	0.55	0.02	0.04	27.5
3	0	0.45	0.02	0.03	22.5
4	5	0.36	0.02	0.03	18.0
5	10	0.51	0.03	0.03	17.0
6	15	0.40	0.03	0.03	13.3
7	25	0.41	0.03	0.03	13.7
8	30	0.30	0.02	0.02	15

In Figure 4.8 it represents the graph where the maximum lift force is 0.55N and minimum 0.30N obtained at -5° and 30° angle of attack. The maximum and minimum drag force is 0.03N and 0.02N at 25° and -5° as well. Where drag force shows a linear graph.

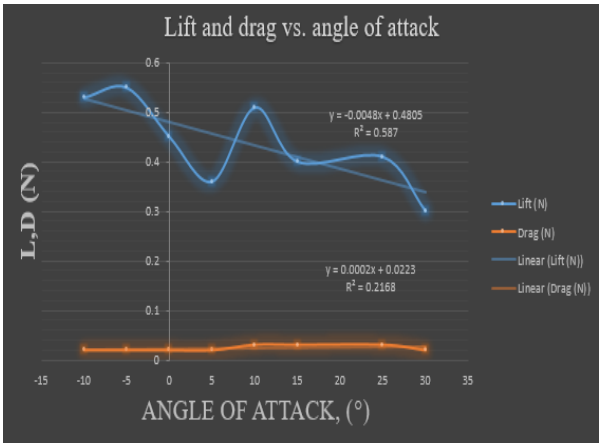


Figure 4.8 lift and drag vs angle of attack at speed 22.33m/s

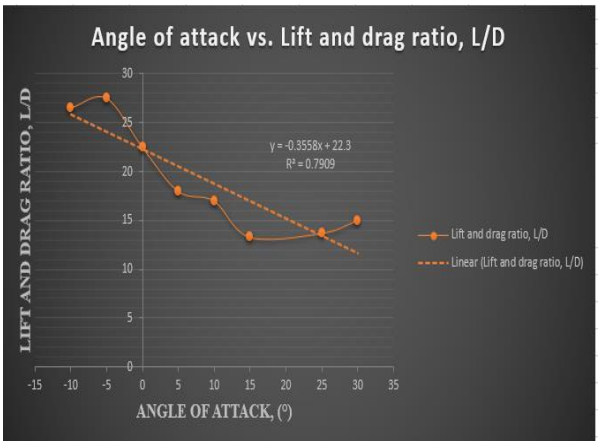


Figure 4.9 Lift and drag ratio vs angel of attack at 22.33m/s

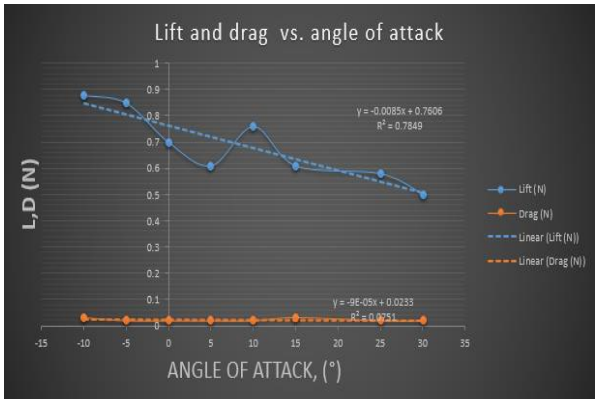
In Figure 4.9 the L/D ratio vs angle of attack graph has been plotted the maximum ratio have obtained 27.5 at -5° and minimum 13.3 at 15°. The ratio is higher between -10° to 10°. It has noticed because of increasing velocity L/D ratio also increasing.

Table 4.3 shows the aerodynamic data at different angle of attack at wind speed 28.83m/s. From there the graphs can be plotted and compare to understating the aerodynamic performances of FHAWT blades.

Table 4.3 Lift and drag force at different angle of attack at wind speed 28.83m/s

No	Angle of attack (°)	Lift (N)	Drag (N)	Pitching moment (Nm)	Lift and drag ratio, L/D
1	-10	0.88	0.03	0.06	29.3
2	-5	0.85	0.02	0.05	42.5
3	0	0.70	0.02	0.04	35.0
4	5	0.61	0.02	0.04	30.5
5	10	0.76	0.02	0.04	38.0
6	15	0.61	0.03	0.04	20.3
7	25	0.58	0.02	0.04	29.0
8	30	0.50	0.02	0.03	25.0

From the graphs which has shown in Figure 4.9 it represents that the maximum lift force created at -10° which is 0.88 and the minimum lift force 0.50N at 30°. Maximum drag force recorded 0.03N at -10° and minimum is 0.02N at -5°.



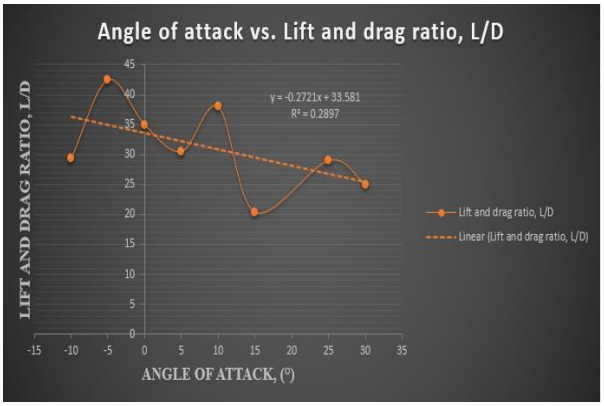


Figure 4.9 Lift and drag vs angle of attack at speed 28.83m/s Figure 4.10 Lift and drag ratio vs angel of attack at 28.83m/s.

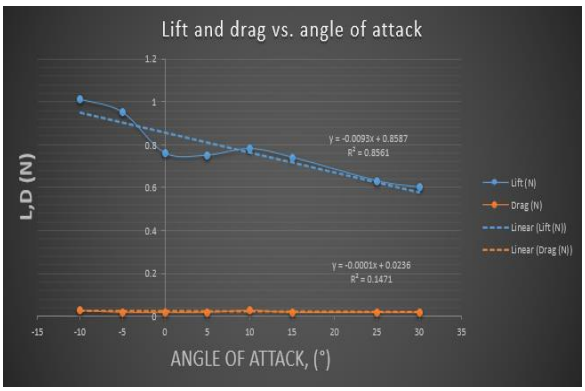
In Figure 4.10 the maximum lift and rag ratio recorded 38 at 10° angle of attack and minimum at 15° angle of attack. The graph shows a sinusoidal characteristic where the ration dropped after 10° angle of attack of the twisted FHAWT blade.

In Table 4.4 lift and drag force, pitching moment and lift and drag ratio has recorded at different angle of attack at wind speed 31.59m/s. where it shows a lot of variant in data because of the change of wind speed which attack the wind turbines blades,

Table 4.4: Lift and drag force at different angle of attack at wind speed 31.59 m/s

No	Angle of attack (°)	Lift (N)	Drag (N)	Pitching moment (Nm)	Lift and drag ratio, L/D
1	-10	1.01	0.03	0.06	33.7
2	-5	0.95	0.02	0.07	47.5
3	0	0.76	0.02	0.05	38.0
4	5	0.75	0.02	0.05	37.5
5	10	0.78	0.03	0.03	26.0
6	15	0.74	0.02	0.05	37.0
7	25	0.63	0.02	0.04	31.5
8	30	0.60	0.02	0.04	30.0

From the graphs which has shown in Figure 4.10 it explains that the maximum lift force created at -10° which is 1.01N and the minimum lift force 0.60N at 30°. Maximum drag force recorded 0.03N at -10° and minimum is 0.02N at -5°.



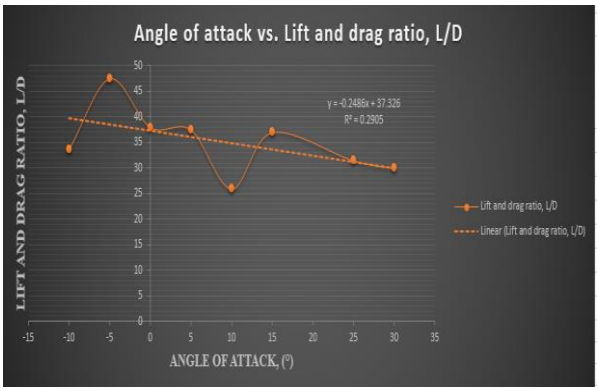


Figure 4.10: Lift and drag vs angle of attack at 31.59m/s Figure 4.11 Lift and drag ratio vs angel of attack at 31.59m/s.

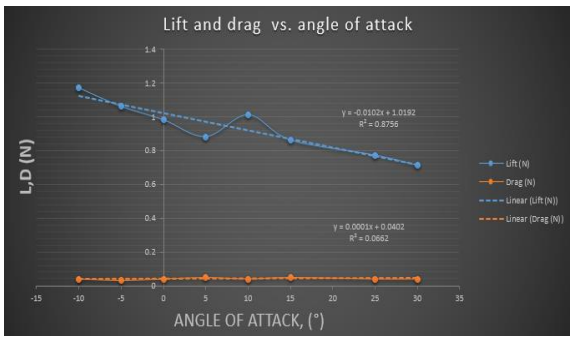
The maximum lift and drag ratio recorded in Figure 4.11 is 47.5 at -5°and minimum 30 at -30°. The ratio is getting higher and proportional to wind velocity. Because of reducing the drag force at different angle the graph shows a sinusoidal line otherwise it could behave like a straight line as there are linear changes of data.

The Table 5.9 shows the tabulated the lift and drag force at different angle of attack at wind speed 36.47m/s. pitching moment and L/D also collected to show the aerodynamic characteristic of the FHAWT blades.

Table 4.5: Lift and drag force at different angle of attack at wind speed 36.47m/s

No	Angle of attack (°)	Lift (N)	Drag (N)	Pitching moment (Nm)	Lift and drag ratio, L/D
1	-10	1.17	0.04	0.05	29.5
2	-5	1.06	0.03	0.07	35.3
3	0	0.98	0.04	0.06	24.5
4	5	0.88	0.05	0.06	17.6
5	10	1.01	0.04	0.06	25.5
6	15	0.86	0.05	0.02	17.2
7	25	0.77	0.04	0.03	19.25
8	30	0.71	0.04	0.03	17.8

From the graphs which has shown in Figure 4.10 it indicates that the maximum lift force created at -10° which is 1.17N and the minimum lift force 0.71N at 30°. Maximum drag force recorded 0.05N at 15° and minimum is 0.03N at -5°. The maximum lift and drag ratio recorded in Figure 4.11 is 35.3 at -5°and minimum 17.6 at 5°. The ratio is high between -10° to 10°. The ration suddenly dropped at 5° which was really unexpected.



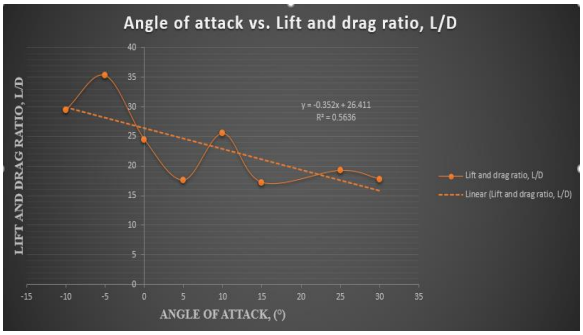


Figure 4.10: Lift and drag vs angle of attack at s36.49m/s Figure 4.11 Lift and drag ratio vs angel of attack at 36.49m/s.

4.3.2 Calculation to Find CL and CD

From lift force CL and CD can be found by using Equation 1 and 2 can rewrite the equation as follows

$L = ½\ C_L\ \rho\ v^2\ A$, $CL=\frac{2L}{\rho V2A}$ …… (3)

And, $D = ½C_D\ \rho\ v^2\ A$,$CD=\frac{2d}{\rho V2A}$…… (4)

Now when,

Air foil section of the blade, $r= 2.48\times10^{-4}$ m, L = lifting force (N) = 1.2N (from experimental data)

D = drag force (N) =0.04 (from experimental data), ρ = density of fluid (kg/m^3) = 1.225 kg/m^3

v = flow velocity (m/s) =36.49 m/s,

A = body area (m^2) $=\pi r^2 = 3.1416 \times(2.48\times10^{-4})^2= 2.48\times10^{-4}$ m^2

C_D = drag coefficient, C_L = lifting coefficient

Then, $CL=\frac{2L}{\rho V2A}=\frac{2x1.2}{1.225x36.5x36.5x7.8x10-4}=1.8$ And $CD=\frac{2d}{\rho V2A}=\frac{2L}{\rho V2A}=\frac{2x0.04}{1.225x36.5x36.5x7.8x10-4}=0.06$

The calculated data has tabulated below:

Table 4.6: Calculated CL and CD at different angle of attack.

No	Angle of attack (°)	Lift (N)	Drag (N)	C_L	CD
1	-10	1.17	0.04	1.8	0.06
2	-5	1.06	0.03	1.61	0.04
3	0	0.98	0.04	1.50	0.06
4	5	0.88	0.05	1.38	0.08
5	10	1.01	0.04	1.58	0.06
6	15	0.86	0.05	1.25	0.08
7	25	0.77	0.04	1.15	0.06
8	30	0.71	0.04	1.05	0.06

4.4 Error calculation and Analysis

To see the errors between simulation and collected experimental data the error calculation has been done with the help of theoretical data which has been obtained in section 4.3.1. the calculation has shown below:

a) Lift force error calculation

The error between theoretical and simulation result

$$\text{Error} = \frac{Experimantal\ value - theoritical\ value}{theoritical\ value} \times 100\%$$

$$= \frac{1.16-1.28}{1.28} \times 100\% = 9.37\%$$

The error between theoretical and wind tunnel test result at 36.49 m/s

$$\text{Error} = \frac{Experimantal\ value - theoritical\ value}{theoritical\ value} \times 100\%$$

$$= \frac{1.1-1.28}{1.28} \times 100\% = 14.6\%$$

b) Drag force error calculation

The error between theoretical and simulation result

$$\text{Error} = \frac{Experimantal\ value - theoritical\ value}{theoritical\ value} \times 100\%$$

$$= \frac{0.05-0.056}{0.056} \times 100\% = 10.71\%$$

The error between theoretical and wind tunnel testing result

$$\text{Error} = \frac{Experimantal\ value - theoritical\ value}{theoritical\ value} \times 100\%$$

$$= \frac{0.04-0.056}{0.056} \times 100\% = 28.57\%$$

Coming to the error analysis among the theoretical, simulation result and wind tunnel testing, it has seen that the error between theoretical and simulation result for lift is around 9.37% and for drag is 10.71%. The data seems very close to each other because in order to validate the result simulation and theoretical calculation has performed. Both process includes mathematical problem and solved by equation. Both process use same method. The difference for theoretical calculated by human and simulation performed by software. That's why the results are very close. On the other hand, the error between theoretical and wind tunnel test result at 36.49 m/s for lift is around 14.6% and drag is 28.57%.

It shows a big difference between the result. The error may have occurred during performing the experiment in the Thermofluids lab in UOW Malaysia KDU University College, Utropolis Glenmarie campus. This error can happen mainly for three reason firstly instrumental error like loose pitot connection, measurement error or the working chamber did not seal properly, secondly environmental error pressure loss between inlet and outlet of wind tunnel while taking reading and the final reason is human error like doing some error be human while doing the testing. The errors have shown to validate the data and the difference. This data is acceptable and seen a slightly difference after comparison in this case.

4.5 Performance analysis between twisted and untwisted blade

4.5.1 Existing untwisted wind turbine blades data

An untwisted wind turbine blade investigation has done in 2015 where it the analysis has carried out in different angle of attack to find out CL and CD. In Figure 4.12 it shows the graphs had been plotted for two different result one is CFD simulation and another one is for Sandia National Laboratory(SANDLA) experimental result [8].

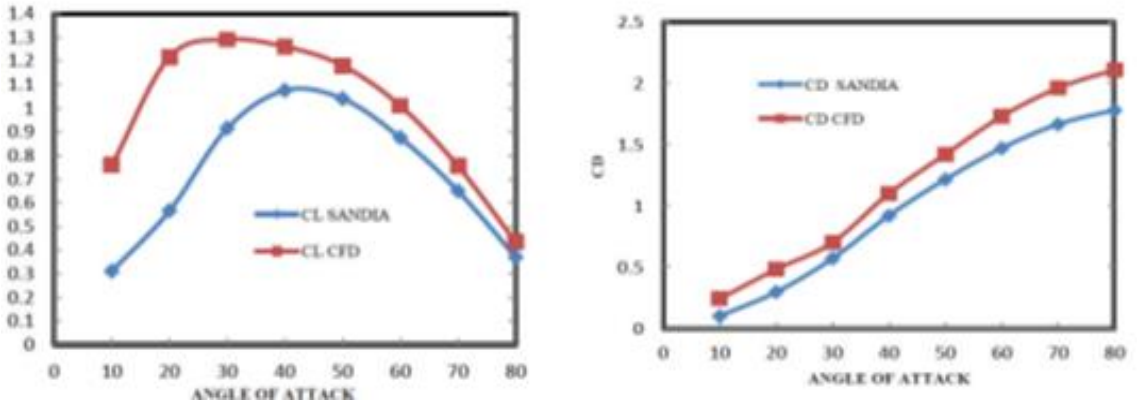


Figure 4.12: CL and CD vs. angle of attack [8]

In 2015 an untwisted air foil based wind turbine blades optimization has done to maximize the L/D ratio. Where they used wind tunnel testing and CFD simulation to analyze it. In Figure 4.13and 4.14 the final result from the investigation has shown where WT180 air foil has been used [9].

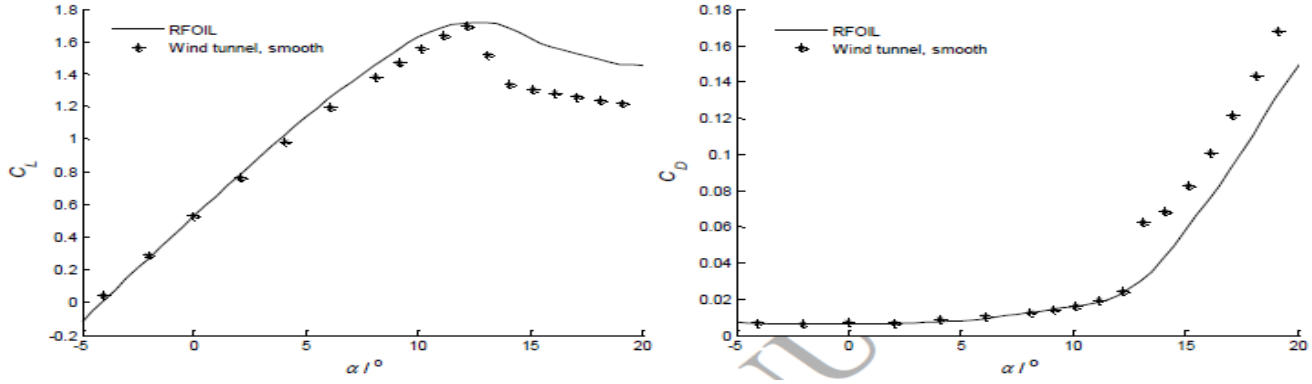


Figure 4.13: CL and CD vs. angle of attack [9]

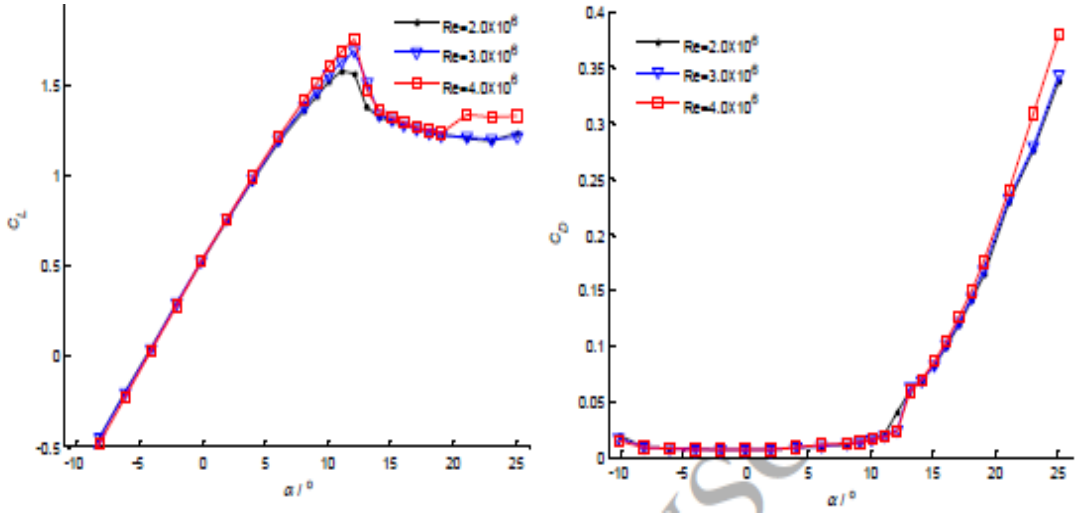
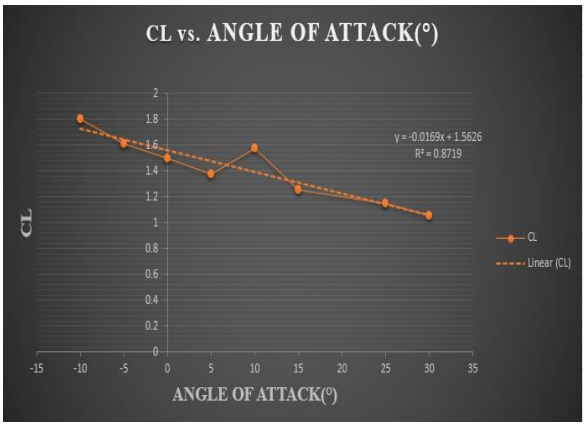


Figure 4.14: CL and CD vs. angle of attack with Re.[10] (Chen et al., 2015)

4.5.2 Designed twisted blade data for FHAWT

The graphs in Figure 4.15 and 4.16 represents the data from Table 4.6 where that graphs have plotted CL vs Angle of Attack to do the comparison between existing untwisted blade and designed FHAWT twisted blade.



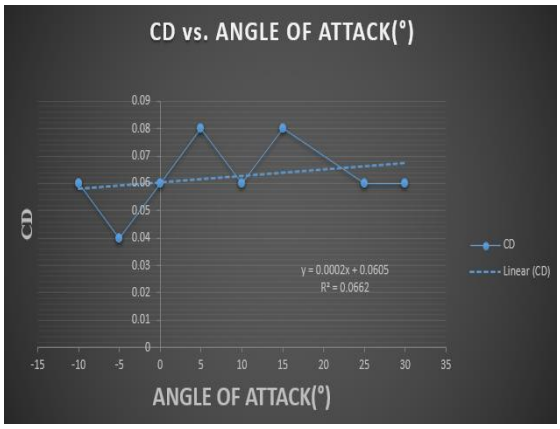


Figure 4.15: CL vs Angle of Attack of designed twisted blades. Figure 4.16:CL vs Angle of Attack of designed twisted blades.

From Figure 4.15 & 4.16 it has seen that maximum CL can get 1.8 at -10° and maximum CD which is 0.06 at -10° as well. The value of CL become lower after 20° and CD started to increase.

4.5.3 Comparison between twisted and untwisted blade

Now coming to the comparison part for untwisted blade two researcher's data has been taken to compare with designed twisted blade data.

At first if notice in Figure 4.12 [8] it can see that the maximum CL can get for the untwisted blade is around 1.05 and maximum drag is around 1.8 and on the other hand, the maximum drag is around 0.6 at 0° to 30° angle of attack. Where twisted blade gives the highest CL is 1.8 and for CD is 0.06 and the lift and ratio will be higher than the untwisted blade. And minimum CL is around 1.01 where the minimum CD is around 0.04 which occurs between -10° to 30° angle of attack.

Figure 4.13 and 4.15 [10] shows that maximum CL and CD between -10° to 20° is 1.14 and 0.17 where the minimum is 0.1 and 0.01. Here the researcher [10] used WT180 which is known as Rfoil [11] though it is good for wind turbine blade but because it is an untwisted blade that's why gives high drag than the designed FHAWT's twisted blade. CL and CD is directly proportional to lift and drag force so the L/D ratio depends on it [12]. Here it has been clearly seen that the L/D ratio for a twisted blade will be higher because of low CD and high CL than untwisted blade.

For a twisted blades of a wind turbine the main magical thing happened is at drag because of in twisted blade the wind can pass easily to reduce the drag force. It has seen that for the twisting angle the drag is reduced almost 10 times than an untwisted blade. So it is clear that twisted blade give better performance than an untwisted blade by reducing drag and increasing lift and drag ratio. Finally, can come to an opinion that twisted blades aerodynamic performances are better than an untwisted blades wind turbine.

4.6 Performance of the twisted FHAWT blade

To see the performance of the designed twisted FHAWT blade need to see the performance of the prototype of FHAWT which has been fabricated after analysing and get the optimization. The offshore environment has been made in the laboratory by using a small swimming pool and industrial fan to give the wind 5m/s to

8m/s. Then all the data has been collected to see the performance. The FHAWT was fabricated in 1/150th Scale to see the performance.

Table 4.7: Performance table of twisted FHAWT.

No	Parameter	Required /Generated
1	Weight of the blade	105.30 g
2	Weight of the FHAWT	1100g
3	Wind velocity	6.5-8 m/s
4	Distance from wind source	662 mm
5	Time to generate electricity	60- 90 s
6	Generated current	0.97 A
7	Generated voltage	0.9V
8	Generated power	0.93W

From Table 4.7 it represents that in 1/150th Scale the performance is quite satisfied. Where targeted shows that the generated power supposed to be 1.01W where the fabricated FHAWT output power found 0.93W which is very close to 1.01W where the difference is around 8%. So it can be stated that the twisted blade will give the maximum power output based on high L/D ratio. Where to obtained high lift and drag force ratio is the main focus of this project. Another thing to get more efficient power the required system components can be added.

CONCLUSION

Finally, it can be concluded that the optimization of the FHAWT blades has achieved which shows high lift and drag ratio than an untwisted blade. Although the FHAWT twisted blade was designed for the variable speed operation in offshore environment it can be applicable for constant speed operation as well. Therefore, velocity is directly proportional to lift and drag where high velocity increases the lift force to spin the blade. Lift and drag ratio increased because twist distribution of the blade by using NACA6409 airfoil. The main difference has observed in twisted blade than untwisted blade is drag where because of twisted blade it reduced almost 10 times. It can be concluded that lift force and co-efficient highly increased when the wind attacks to the blades between -10° to 20°. The lift gets higher most at -10° and 10° angle of attack because the wind can attack directly at the edge of twisted blade to generate the lift force. The best place in offshore to capture the energy should be investigating to reduce the waste of energy. An evaluation of rotor, hub and nacelle should be done to optimize the FHAWT at different angle of attack and wind speed.

REFERENCES

1) C. E. Commission, “2012 ACCOMPLISHMENTS Adopting first-in-the-nation efficiency,” no. Title 24, pp. 1–8, 2013.
2) M. B. Alawi, “The integration of wind turbines for generating sustainable energy in skyscrapers,” no. May, pp. 0–13, 2019.
3) K. Cox and A. Echtermeyer, Structural design and analysis of a 10MW wind turbine blade, vol. 24, no. 1876. 2012.
4) S. Butterfield, “Aiaa 2004-1007 feasibility of floating platform systems for wind turbines,” no. January, 2004.
5) Airfoil Tools, “NACA6409 9% (n6409-il),” 1636 airfoils, 2016. [Online]. Available: http://airfoiltools.com/airfoil/details?airfoil=n6409-il.
6) K. Prasad, B. A. Prasad, and M. Anandarao, “Optimization of Twisted Aero-Foil Blade Angle of a

Structural Gas Turbine Assembly," vol. 12, no. 15, pp. 4818–4824, 2017.

7) M. J. Kirsch, "DESIGN OF A SMALL WIND TURBINE FOR ELECTRIC POWER GENERATION (1-5kW)," no. November, 2009.
8) H. R. T. Bhushan S. Patil, "conmputational fluid dynamics analysis of wind turbine blade," vol. 127, pp. 1363–1369, 2015.
9) J. Chen, Q. Wang, S. Zhang, P. Eecen, and F. Grasso, "PT US CR," Appl. Math. Model., 2015.
10) M. Rahman, Z. Chao, W. T. Chong, S. Julai, and S. Y. Khoo, "Performance enhancement of wind turbine systems with vibration control : A review," vol. 51, pp. 43–54, 2015.
11) F. Hossain, A. Morshed, R. Sultana, and Q. Islam, "Measurement of Flow Rate and Impact Force on Different Vanes through Impact of Jet Measurement of Flow Rate and Impact Force on Different Vanes through Impact of Jet," no. July, 2018.
12) V. Mendoza, Aerodynamic Studies of Vertical Axis Wind Turbines using the Actuator Line Model. 2018.